Original Article
ISSN (Online): 2582-7472

ShodhKosh: Journal of Visual and Performing Arts
July-December 2023 4(2), 5934–5946

COMPUTATIONAL ANALYSIS OF CONVECTIVE HEAT AND MASS TRANSFER FLOW OF SECOND GRADE FLUID WITH CHEMICAL REACTION

N. Srinivasa Rao [1]

[1] Associate Professor, Department of Mathematics, GFGC, Kolar, Karnataka, India

Corresponding Author

N. Srinivasa Rao,
n.s.s.rao2526@gmail.com

DOI

10.29121/shodhkosh.v4.i2.2023.6378

Funding: This research received no specific grant from any funding agency in the public, commercial, or not-for-profit sectors.

ABSTRACT

In the present paper, we investigate the effect of chemical reaction the heat generating on the unsteady free convection MHD gyrating flow of radiation and chemical reactive second grade discussed. Here, it is assumed that, the confining plate has the ramped wall temperature with ramped surface concentration and isothermal temperature with ramped surface concentration. The non-linear coupled equations governing the flow, heat and mass transfer are solved numerically by Galerkin Finite Element Analysis. In addition to the idioms of skin friction, Nusselt fluid past an unbounded perpendicular plate during absorbent medium have been number as well as Sherwood number are achieved and characterized numerically with tabular format.

Keywords: Chemical Reaction, Porous Medium, Heat and Mass Transfer, Second Grade Fluid

1. INTRODUCTION

The study of combined heat and mass transfer problems has great importance in extending theory of separation processes, chemical and hydro-metallurgical industries. Heat transfer phenomenon in addition to the mass transfer has received great attention of modern researchers for its enormous applications in chemical industries, reservoir engineering and other processes. A few representation fields of this type of flows in which combined heat and mass transfer with chemical reaction effect plays an important role, are electrical energy is extracted directly from a moving conducting fluid, formation and dispersion of fog, damage of crops due to freezing, distribution of temperature and moisture over groves of fruit trees, manufacturing of ceramics, polymer production.Tan and Masuoka [1] found the Stokes first problems for the second graded fluids and Rashidi et al. [2] discussed by the unsteady compressible flows of the second order fluids. Hayat et al. [3] explored by the unsteady stagnation point flow of second grade fluids with changeable free stream. Due to complicated relation between stress and strain in non- Newtonian fluids and their technological application, their study in fluid dynamics is more valuable than Newtonian fluids. Viscous fluids flow has

attracted the attention of scientists and engineers because of its important applications notably in the flow of oil through porous rocks, the extraction of energy from geothermal regions, the filtration of solids from liquids and drug penetration through human skin. Second grade fluid is a subclass of non-Newtonian fluid in which velocity field has up to two derivatives in stress strain tensor relationship where as in Newtonian fluid it has derivatives up to first order. Flow of second grade fluid gains attention of the researchers in many boundary layer flows and have been successfully studied in various kinds of flows. Study of heat transfer in non-Newtonian fluids is much interesting for researchers now-a-days. The magneto hydrodynamic (MHD) is a subdivision of fluid dynamics and this studied the association of the electrically conducting fluids in the magnetic field. Many of investigative efforts in the MHD has been proceed extensively for the duration of the preceding little decades subsequent to the established work of Hartmann [4] in fluid metalized ducts flow under external magnetic field. There are most applications for the parabolic movement for instance solar cooker, solar concentrator and parabolic through stellar collector. The parabolic concentrator model solar cookers have the wide range of applications for example baking, roast as well as distillations. Solar concentrator model had those applications into growing rates of evaporations in dissipate stream, in food dispensations, for producing consumption water from salt water as well as seawater. Murthy et al. [5] discussed by the evaluations of thermal performances of temperature exchangers units for parabolic solar cookers. Raja et al. [6] explored the designing as well as manufacturing of parabolic during solar collector systems. Muthucumaraswamy and Geetha [7] discussed the impacts of parabolic movement on the isothermal perpendicular plates by the invariable mass flux. Akbar et al. [8] considered the MHD stagnation point flow of Carreau fluid towards the porous shrinking sheet. Sheikholeslami et al. [9] discussed the magnetic field effects on nanofluids flows as well as temperature transportation. Magnetic field effects on unsteady nanofluids flows as well as temperature transportation utilizing the Buongiornos modeling has been discussed by Sheikholeslami et al. [10]. Sheikholeslami et al. [11] explored the unsteady MHD liberated convective stream in the eccentrics semi-annulus packed by the nanofluids. Sheikholeslami as well as Ellahi [12] explored the 3D meso-scopic simulation of magnetic field effects on nanoliquids. Sheikholeslami et al. [13] defined the solution of forced convective temperature transportation by the changeable magnetic fields. Sheikholeslami and Chamkha [14] studied the free convective temperature transportation of the nanoliquids into the half-annulus enclosures by the sinusoidal walls. Recently, Krishna and Chamkha [15] explored the diffusion-thermo effect, radiating-absorptions, Hall as well as ion slip impacts on the MHD liberated convection gyratory flows of the nanofluids past the semi-infinite permeable inspiring plate with the unchanging temperature sources. The impacts of radiating as well as Hall currents on the unsteady MHD liberated central heating flows into the perpendicular channel/duct packed by the absorbent media has been explored by Krishna et al. [16]. The temperature generating/absorption as well as thermo-diffusions on the unsteady complimentary convection MHD flows of radiation as well as the chemical reactive second grade liquid past an unbounded perpendicular plate during the absorbent media as well as considering the Hall current into accounts had been considered by Krishna and Chamkha [17]. Thermal radiation constraint impacts might do the significant roles in scheming temperature transportation into the polymer processing industries. Numerous investigators similar to, Sheikholeslami et al. [18] the impact of thermal radiating on unsteady MHD nanofluids stream as well as temperature transport through two phase modeling. Krishna et al. [19] explored the temperature as well as mass transport on unsteady MHD oscillating flows of second grade liquid during a permeable media between two perpendicular plates under the influences of unpredictable temperature resource and/or sink, as well as chemically reacting. Kataria and Mittal [20] has explored the effects of thermally radiating impacts on nanoliquids flow. Nadeem et [21] investigated the MHD three dimensional Casson fluids movement over the permeable linearly stretching sheet. Kataria and Mittal [22] discussed the velocity, mass as well as temperature transportation analysis of free/forced convective nanofluids flow over on fluctuating perpendicular plate with magnetic field embedded in an absorbent medium.

Keeping the above mentioned facts, on the unsteady free convection MHD gyrating flow of radiation and chemical reactive second grade fluid over an unbounded perpendicular plate during absorbent medium have not been discussed yet. Therefore, novelty of the current paper is that, the heat generating and/or absorption as well as thermo-diffusion on the unsteady free convection MHD gyrating flow of radiation and chemical reactive second grade fluid over an unbounded perpendicular plate during absorbent medium have been discussed.

2. MATHEMATICAL ANALYSIS

We consider the steady two-dimensional laminar boundary layer flow of a viscous, electrically conducting and heat absorbing fluid past a semi-infinite vertical plate embedded in a porous medium which is subjected to thermal and

concentration buoyancy effects. We choose a rectangular coordinates O(x,y) with x-aixs along the plate and y-axis normal to the plate. The plate is maintained at constant temperature Tw and concentration Cw higher than ambient temperature T∞ and concentration C∞ respectively. Also we assume that there exists a homogeneous chemical reaction of first-order with constant rate k1 between the diffusing species and the fluid.

The concentration of the diffusing species is very small in comparison to other chemical species, the concentration of the species far away from the wall C∞, is infinitesimally small and hence the soret and dufour effects are neglected. The chemical reactions are taking place in the flow and all thermo-physical properties are assumed to be constant except density in the buoyancy terms of the linear momentum equation which is approximated according to the Boussinesq approximation. A uniform magnetic field B is applied transverse to the plate. Assuming the magnetic Reynolds number to be small we neglect the induced magnetic field and Hall effects. It is assumed that the porous medium is homogeneous and present energy where in local thermodynamic equilibrium. Under these approximations the boundary layer free convection flow, heat and mass transfer motions are

$$\frac{\partial v^*}{\partial y^*} = 0 \tag{2.1}$$

$$\frac{\partial p^*}{\partial y^*} = 0 \Rightarrow p^* \text{ is independent of } y^* \tag{2.2}$$

$$\rho v^* \frac{\partial u^*}{\partial y^*} = \mu \frac{\partial^2 u^*}{\partial y^{*2}} - \frac{\mu}{K^*} u^* - \sigma B_0^2 u^* + \rho g \beta_T (T^* - T_\infty) + \rho g \beta_C (C^* - C_\infty) \tag{2.3}$$

$$\rho C_p v^* \frac{\partial T^*}{\partial y^*} = K_f \frac{\partial^2 T^*}{\partial y^{*2}} + \mu \left(\frac{\partial u^*}{\partial y^*} \right)^2 - \frac{\partial q_r^*}{\partial y^*} + \sigma B_0^2 u^{*2} - Q_0 (T^* - T_\infty) + Q_1 (C^* - C_\infty) \tag{2.4}$$

$$v^* \frac{\partial C^*}{\partial y^*} = D \frac{\partial^2 C^*}{\partial y^{*2}} - K_1 (C^* - C_\infty) \tag{2.5}$$

Where (i.e., is constant the components of dimensional velocities along and directions. is the fluid thermal diffusivity. The fourth and fifth terms on RHS of the momentum equation (2.3) denote the thermal and concentration buoyancy effects, respectively. Also, second and fourth terms on RHS of energy equation (2.4) denote the viscous and Ohmic dissipations respectively and third, fifth and sixth terms on RHS of (2.4) denote inclusion of the effect of thermal radiation heat source and radiation absorption effects respectively.

The radiative heat flux is given by

$$\frac{\partial q_r^*}{\partial y^*} = 4(T^* - T_\infty) I' \tag{2.6}$$

where $I' = \int_0^\infty K_{\lambda w} \frac{\partial e_{b\lambda}}{\partial T^*} d\lambda$, $K_{\lambda w}$ is the absorption coefficient at the wall and is Planck's function.

The appropriate boundary conditions for velocity, temperature and concentration fields are

$$\begin{aligned} &y^* = 0 : u^* = 0,\ T^* = T_w,\ C^* = C_w \\ &y^* \to \infty : u^* \to 0,\ T^* \to T_\infty,\ C^* \to C_\infty \end{aligned} \tag{2.7}$$

where and are the wall dimensional concentration and temperature respectively.

The equation (2.2)-(2.5) are coupled, parabolic and non-linear partial differential equations and hence analytical solution is not possible. Therefore, numerical technique is employed to obtain the required solution. Numerical computations are greatly facilitated by non-dimensionalization of the equations. In order to write governing equations and boundary conditions in dimensionless form, the following non-dimensionless quantities are introduced.

$$y = \frac{v_0 y^*}{v},\ u = \frac{u^*}{v_0},\ M^2 = \frac{B_0^2 v^2 \sigma}{v_0^2 \mu},\ K = \frac{K^* v_0^2}{v^2},\ \theta = \frac{T^* - T_\infty}{T_w - T_\infty},\ C = \frac{C^* - C_\infty}{C_w - C_\infty}. \tag{2.8}$$

we get the following non-dimensional equations:

$$\frac{d^2u}{dy^2}+\frac{du}{dy}-(M^2+D^{-1})u=-G(\theta+NC) \qquad (2.9)$$

$$\frac{d^2\theta}{dy^2}+\Pr\frac{d\theta}{dy}+\Pr E\left(\frac{du}{dy}\right)^2-\Pr(R+\alpha)\theta+\Pr EcM^2u^2+Q_1C=0 \qquad (2.10)$$

$$\frac{d^2C}{dy^2}+Sc\frac{dC}{dy}-ScKC=0 \qquad (2.11)$$

where G is the Grashof number, N is the Buoyancy ratio, Pr is the Prandtl number, M is the magnetic field parameter, R is the radiation parameter, Sc is the Schmidt number, Ec is the Eckert number, is the heat source parameter, and is the chemical reaction parameter D-1 is the Darcy parameter and Q1 is the radiation absorption parameter defined as follows:

$$Ec=\frac{v_0^2}{C_p(T_w-T_\infty)},\quad \Pr=\frac{\mu C_p}{K_f},\quad G=\frac{\rho g\beta_T v^2(T_w-T_\infty)}{v_0^3\mu},\quad Sc=v/D,\quad R=\frac{4vI'}{\rho C_p v_0^2},$$

$$N=\frac{\beta_T(C_w-C_\infty)}{\beta_C(T_w-T_\infty)},\quad K=\frac{Rv}{v_0^2},\quad \alpha=\frac{Q_0v}{\rho C_p v_0^2},\quad Q_1=\frac{Q_1(C_w-C_\infty){v_0}^2}{(T_w-T_\infty)v^2}$$

The corresponding boundary condition in dimensionless form is

$$y=0:\ u=0,\ \theta=1,\ C=1$$
$$y\to\infty:\ u\to0,\theta\to0,\ C\to0. \qquad (2.12)$$

For the type of flow under consideration, the physical quantities such as the wall shear stress, surface heat flux and the surface mass flux are very important, which are given by

$$\tau_w=\mu\left(\frac{\partial u}{\partial y}\right)_{y=0}$$

$$q_w=-k\left(\frac{\partial T}{\partial y}\right)_{y=0}$$

$$M_w=-D\left(\frac{\partial C}{\partial y}\right)_{y=0}$$

where is the viscosity and k is the thermal conductivity.

Hence, the skin-friction coefficient, Nusselt number and Sherwood number near the plate in non-dimensional form are given by

$$C_f=\frac{\tau_w}{\rho{v_0}^2}=u'(0)$$

$$\frac{Nu_x}{\mathrm{Re}_x}=\frac{q_wx}{k(T_w-T_\infty)}=-\theta'(0)$$

$$\frac{Sh_x}{\mathrm{Re}_x}=\frac{M_wx}{D(T_w-T_\infty)}=-C'(0)$$

where $\mathrm{Re}_x = \frac{v_0 x}{v}$ is local Reynolds number.

3. METHOD OF SOLUTION

The set of coupled non-linear governing boundary layer equations (2.1)-(2.5) together with the boundary conditions (2.7) are solved numerically by using Galerkin Finite Element Analysis. The finite element method is a powerful technique for solving differential or partial differential equations as well as for integral equations. This method is so general that it can be applied even for integral equations including heat transfer fluid mechanics, solid mechanics, electrical systems, chemical processing and other fields also. From the process of numerical computation, the skin-friction coefficient, the Nusselt number and the Sherwood number, which are respectively proportional to are also sorted out and their numerical valued are presented in a tabular form.

4. FINITE ELEMENT ANALYSIS & FORMULATION

The finite element analysis with quadratic polynomial approximation function is carried out along the axial distance. The behavior of the velocity, temperature and concentration profiles has been discussed computationally for different variations in governing parameters. The Galerkin method has been adopted in the variational formulation in each element to obtain the global coupled matrices for the velocity, temperature and concentration in course of the finite element analysis.

Without loss of generality ∞ has been shifted at $\eta = 6$ for the computational purposes. The domain is divided into a set of line elements (say N), each element having three end nodes.

Choose an arbitrary element e_k and let u^k, θ^k and be the values of u, θ and in the element e_k .

We define the error residuals as

$$E_u^k = \frac{d}{d\eta}\left(\frac{\mathrm{du}^{\mathrm{k}}}{d\eta} + u^k\right) - (M^2 + D^{-1})u^k + G(\theta^k + NC^k) \qquad (3.1)$$

$$E_\theta^k = \frac{d}{d\eta}\left(\frac{d\theta^k}{d\eta}\right) + \mathrm{Pr}\frac{d\theta^k}{d\eta} + \mathrm{Pr}\,Ec\left(\frac{du^k}{d\eta}\right)^2 - \mathrm{Pr}(R+\alpha)\theta^k + P_r EcM^2\left(u^k\right)^2 + Q_1 C^k \qquad (3.2)$$

$$E_c^k = \frac{d}{d\eta}\left(\frac{dC^k}{d\eta}\right) + Sc\frac{dC^k}{d\eta} - ScKC^k \qquad (3.3)$$

where u^k, θ^k & C^k are the values of u, θ & C in the arbitrary element e_k.

The finite element approximations of u^k, θ^k & C^k are taken as,

$$\begin{aligned} u^k &= u_1^k \Psi_1^k + u_2^k \Psi_2^k + u_3^k \Psi_3^k \\ \theta^k &= \theta_1^k \Psi_1^k + \theta_2^k \Psi_2^k + \theta_3^k \Psi_3^k \\ C^k &= C_1^k \Psi_1^k + C_2^k \Psi_2^k + C_3^k \Psi_3^k \end{aligned} \qquad (3.4)$$

For a typical element, the interpolation functions (Shaped functions) are given by

$$\Psi_1^k = \frac{\left(\eta - \frac{2k-1}{n}s\right)\left(\eta - \frac{2k}{n}s\right)}{s\left(\frac{2k-2}{n} - \frac{2k-1}{n}\right)s\left(\frac{2k-2}{n} - \frac{2k}{n}\right)}$$

$$\Psi_2^k = \frac{\left(\eta - \frac{2k-2}{n}s\right)\left(\eta - \frac{2k}{n}s\right)}{s\left(\frac{2k-1}{n} - \frac{2k-2}{n}\right)s\left(\frac{2k-1}{n} - \frac{2k}{n}\right)}$$

$$\Psi_3^k = \frac{\left(\eta - \frac{2k-1}{n}s\right)\left(\eta - \frac{2k-2}{n}s\right)}{s\left(\frac{2k}{n} - \frac{2k-2}{n}\right)s\left(\frac{2k}{n} - \frac{2k-1}{n}\right)}$$

where Ψ_1^k, Ψ_2^k & Ψ_3^k are Lagrange□s quadratic polynomials, $k = \frac{n}{2}$ & $s = 6$. Following the Galerkin weighted residual method and integrating (3.1)-(3.3), we obtain

$$\int_{\eta_e}^{\eta_e+1} \frac{du^k}{d\eta}\frac{d\Psi_j^k}{d\eta}d\eta - \int_{\eta_e}^{\eta_e+1} \frac{du^k}{d\eta}\Psi_j^k d\eta + (M^2 + D^{-1})\int_{\eta_e}^{\eta_e+1} u^k \Psi_j^k d\eta$$

$$- G\int_{\eta_e}^{\eta_e+1} (\theta^k + NC^k)\Psi_j^k d\eta = Q_{2j} + Q_{1j} \qquad (3.5)$$

where $Q_{2j} = \left((\frac{du^k}{d\eta} + u^k)\Psi_j^k\right)_{\eta_e+1}$ & $-Q_{1j} = \left((\frac{du^k}{d\eta} + u^k)\Psi_j^k\right)_{\eta_e}$

$$\int_{\eta_e}^{\eta_e+1} \frac{d\theta^k}{d\eta}\frac{d\Psi_j^k}{d\eta}d\eta - \Pr\int_{\eta_e}^{\eta_e+1} \frac{d\theta^k}{d\eta}\Psi_j^k d\eta - \Pr Ec\int_{\eta_e}^{\eta_e+1}\left(\frac{du^k}{d\eta}\right)^2 \Psi_j^k d\eta + \Pr(R+\alpha)\int_{\eta_e}^{\eta_e+1} \theta^k \Psi_j^k d\eta$$

$$- \Pr EcM^2\int_{\eta_e}^{\eta_e+1} \left(u^k\right)^2 \Psi_j^k d\eta + Q_1\int_{\eta_e}^{\eta_e+1} C^k \Psi_j^k d\eta = S_{2j} + S_{1j} \qquad (3.6)$$

$$\int_{\eta_e}^{\eta_e+1} \frac{dC^k}{d\eta}\frac{d\Psi_j^k}{d\eta}d\eta - Sc\int_{\eta_e}^{\eta_e+1} \frac{dC^k}{d\eta}\Psi_j^k d\eta + ScK\int_{\eta_e}^{\eta_e+1} C^k \Psi_j^k d\eta = R_{2j} + R_{1j} \qquad (3.7)$$

where $R_{2j} = \left(\frac{dC^k}{d\eta}\Psi_j^k\right)_{\eta_e+1}$ & $-R_{1j} = \left(\frac{dC^k}{d\eta}\Psi_j^k\right)_{\eta_e}$

Substituting in terms of local nodal values, the above equations (3.6)-(3.9) reduces to

$$\sum_{i=1}^{3} u_i^k \int_{\eta_e}^{\eta_e+1} \frac{d\Psi_i^k}{d\eta}\frac{d\Psi_j^k}{d\eta}d\eta - \sum_{i=1}^{3} u_i^k \int_{\eta_e}^{\eta_e+1} \frac{d\Psi_i^k}{d\eta}\Psi_j^k d\eta + (M^2 + D^{-1})\sum_{i=1}^{3} u_i^k \int_{\eta_e}^{\eta_e+1} \Psi_i^k \Psi_j^k d\eta$$

$$- G\sum_{i=1}^{3} (\theta_i^k + NC_i^k)\int_{\eta_e}^{\eta_e+1} \Psi_i^k \Psi_j^k d\eta = Q^k{}_{2j} + Q^k{}_{1j} \qquad (3.8)$$

$$\sum_{i=1}^{3} \theta_i^k \int_{\eta_e}^{\eta_e+1} \frac{d\Psi_i^k}{d\eta}\frac{d\Psi_j^k}{d\eta}d\eta - \Pr\sum_{i=1}^{3} \theta_i^k \int_{\eta_e}^{\eta_e+1} \frac{d\Psi_i^k}{d\eta}\Psi_j^k d\eta - \Pr Ec\sum_{i=1}^{3} u_i^k \int_{\eta_e}^{\eta_e+1}\left(\frac{du^k}{d\eta}\right)^2 \Psi_j^k d\eta$$

$$+ \Pr(R+\alpha)\sum_{i=1}^{3} \theta_i^k \int_{\eta_e}^{\eta_e+1} \Psi_i^k \Psi_j^k d\eta - \Pr EcM^2\sum_{i=1}^{3} u_i^k \int_{\eta_e}^{\eta_e+1} \left(\Psi_i^k\right)^2 \Psi_j^k d\eta$$

$$+Q_1\sum_{i=1}^{3}C_i^k\int_{\eta_e}^{\eta_e+1}\left(\Psi_i^k\right)^2\Psi_j^k d\eta = S^k{}_{2j}+S^k{}_{1j} \quad (3.9)$$

$$\sum_{i=1}^{3}C_i^k\int_{\eta_e}^{\eta_e+1}\frac{d\Psi_i^k}{d\eta}\frac{d\Psi_j^k}{d\eta}d\eta - Sc\sum_{i=1}^{3}C_i^k\int_{\eta_e}^{\eta_e+1}\frac{d\Psi_i^k}{d\eta}\Psi_j^k d\eta + ScK\sum_{i=1}^{3}C_i^k\int_{\eta_e}^{\eta_e+1}\Psi_i^k\Psi_j^k d\eta = R_{2j}+R_{1j} \quad (3.10)$$

Choosing Ψ_j^k s corresponding to each element e_k in the equation (3.9) yields a local stiffness matrix of order in the form

$$\left(f_{ij}^k\right)\left(u_i^k\right)-\left(g_{ij}^k\right)\left(u_i^k\right)+(M^2+D^{-1})\left(h_{ij}^k\right)\left(u_i^k\right)-G\left(K_{ij}^k\right)\left(u_i^k\right)=\left(Q_{2j}^k\right)+\left(Q_{1j}^k\right)+\left(v_j^k\right) \quad (3.11)$$

Likewise the equation (22) & (23) gives rise to stiffness matrices

$$\left(m_{ij}^k\right)\left(\theta_i^k\right)-\Pr\left(n_{ij}^k\right)\left(\theta_i^k\right)-\Pr Ec\left(o_{ij}^k\right)\left(u_i^k\right)+\Pr(R+\alpha)\left(p_{ij}^k\right)\left(\theta_i^k\right)-\Pr EcM^2\left(q_{ij}^k\right)\left(\theta_i^k\right)+Q_1\left(r_{ij}^k\right)\left(C_i^k\right)=\left(S_{2j}^k\right)+\left(S_{1j}^k\right)+\left(v_j^k\right) \quad (3.12)$$

$$\left(s_{ij}^k\right)\left(C_i^k\right)-Sc\left(t_{ij}^k\right)\left(C_i^k\right)+ScK\left(x_{ij}^k\right)\left(u_i^k\right)=\left(R_{2j}^k\right)+\left(R_{1j}^k\right)+\left(v_j^k\right) \quad (3.13)$$

Where $\left(f_{1j}^k\right),\left(g_{1j}^k\right),\left(h_{1j}^k\right),\left(K_{1j}^k\right),\left(m_{1j}^k\right),\left(n_{1j}^k\right),\left(o_{1j}^k\right),\left(p_{1j}^k\right),\left(q_{1j}^k\right),\left(r_{1j}^k\right),\left(s_{1j}^k\right),\left(t_{1j}^k\right),\left(x_{1j}^k\right)$ are matrices and $v_j^k=-A\int_{\eta_e}^{\eta_e+1}\Psi_i^k\Psi_j^k d\eta$ and, $\left(Q_{2j}^k\right),\left(Q_{1j}^k\right),\left(S_{2j}^k\right),\left(S_{1j}^k\right),\left(R_{2j}^k\right),\left(R_{2j}^k\right)$ are column matrices and such stiffness matrices (3.11)-(3.13) in terms of local nodes in each element are assembled using inter element continuity and equilibrium conditions to obtain the coupled global matrices in terms of the global nodal values of u, θ & C. The whole domain is divided into a set of 100 line elements equations we obtain a matrix of order 201×201. This system of equations as obtained after assembly of the elements equations is non-linear therefore an iterative scheme has been used to solve it. The system is linearized by incorporating known functions. After applying the given boundary conditions only a system of 195 equations remains for the solution which has been solved using Gauss elimination method. Convergence is assumed when the ratio of every one of u^k, θ^k & C^k for last 2 approximations differed from unity by less than 10-5 at all values of in $0<\eta<\eta_\infty$. It should be mentioned that the results obtained herein reduce to those reported by D.Pal(2010) when Q1=0, which gives validity of the present solution provided in Tables 1 &2.

5. ANALYSIS OF NUMERICAL RESULTS

As a result of the numerical calculations, the dimensionless velocity, temperature and concentration distribution for the flow under consideration are obtained and their behavior has been discussed for variations in the governing parameters. In the present study we adopted the following default parameter values of finite element method: G=4, M=2, N=0.5, D-1=2, Pr=0.71, Ec=0.0001, R=3, Sc=0.6, K=0.5, =2, Q¬1=0.5. All graphs therefore correspond to these values unless specifically indicated on the appropriate graph.

The influence of radiation of heat flux on u is shown in fig-1. It is found that higher the radiation parameter R, smaller the velocity u which shows that an increase in the radiation parameter R decreases the velocity in boundary layer due to decrease in the boundary layer thickness. Fig-2 represents the variation of u with buoyancy ratio N. It is found that when the molecular buoyancy force dominates over the thermal buoyancy force, the velocity experiences an enhancement when the buoyancy forces act in the same direction and for the forces acting in opposite directions we notice a depreciation in the velocity u. Fig-3 represents the velocity with rate of chemical reaction parameter K. It is found that the velocity depreciates in the degenerating chemical reaction case (K>0) and in the generating chemical reaction case, we find that u experiences an enhancement in the boundary layer. Hence increase in K>0 leads to a fall in the momentum boundary layer and an increase in K<0 leads to rise in the momentum boundary layer. Fig.4 represents with radiation parameter R. An increase in the radiation parameter R leads to a depreciation in the thermal boundary layer thickness and thereby reducing the heat transfer in the flow region. The variation of with chemical reaction

parameter K is shown in fig.5 It is found that the temperature depreciates in the degenerating chemical reaction case and enhances in the generation chemical reaction case. Fig.6 represents the variation of with radiation absorption parameter Q1. It is found that the temperature increases with increase in Q1. This is due to the fact that an increase in Q1 results in an enhancement in in the vicinity of surface y=0. The variation of C with chemical reaction parameter K is shown in fig.7 This shows that the concentration decreases in the degenerating chemical reaction case and enhances in the generating chemical reaction case. This is due to the fact that the thickness of the boundary layer decreases with increase in the value K>0. i.e., chemical reaction in this system results in the consumption of chemical and hence results in concentration profile to decrease. In the case of K<0 i.e., chemical reaction in this system results in the emission of the chemical and hence results in the concentration profiles to increase in the boundary layer. The variation of Cfx with chemical reaction parameter is shown in fig.8. We notice that the concentration depreciates in the degenerating chemical reaction case. Fig.9 represents Nux with chemical reaction parameter K. We notice from this figure that the local nusselt number Nux experience in an enhancement with increase in K. Thus, Nux enhances in the degenerating chemical reaction case.

From Tables.1 and 2 The actual concentration reduces with increase in Sc, also it depreciates with increase in K>0 and enhances with K<0.The local skin-friction coefficient Cfx reduces with increase in M or Sc or chemical reaction parameter K.The local Nusselt number Nux experiences in an enhancement with increase in Sc, , Q1 and K, and reduces in M.The rate of mass transfer at y=0 enhances with increase in Sc and K>0 and depreciates in the generating chemical reaction c<0.as K

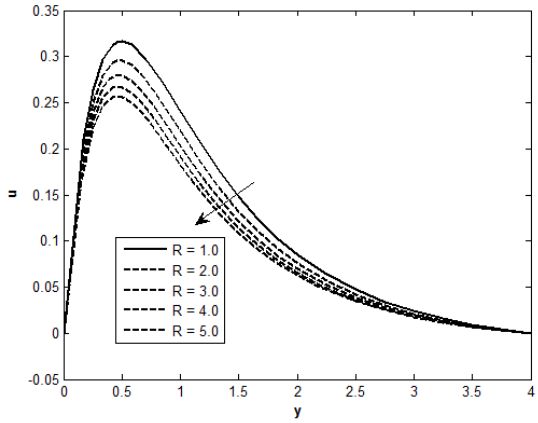

Figure 1 Velocity profiles for various values of R.

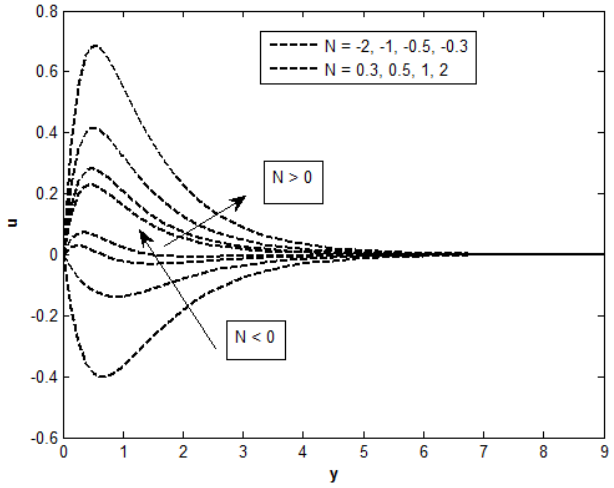

Figure 2 Velocity profiles for various values of N.

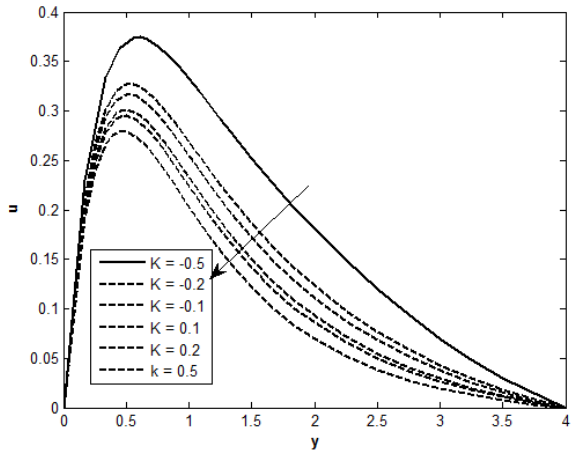

Figure 3 Velocity profiles for various values of K.

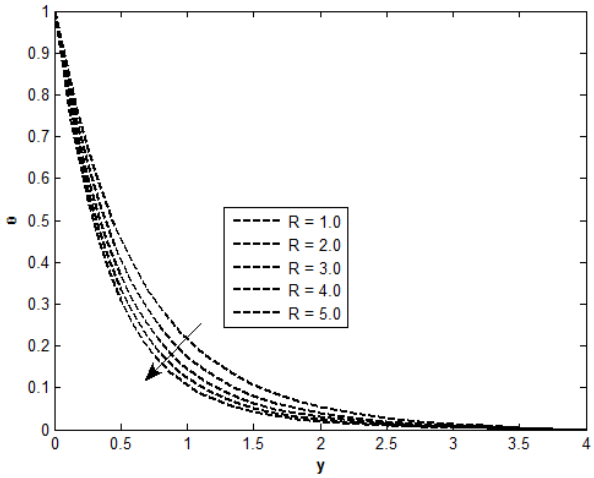

Figure 4 Temperature distribution for various values of R.

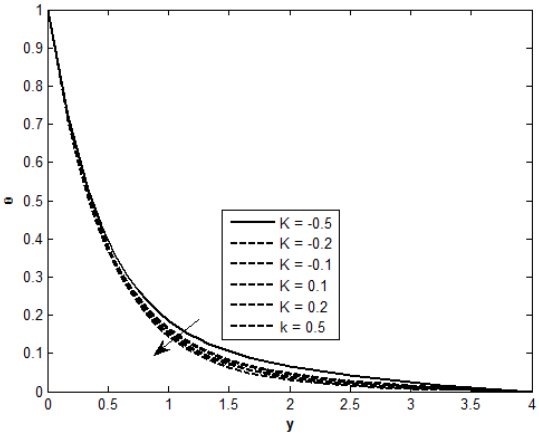

Figure 5 Temperature distribution for various values of K.

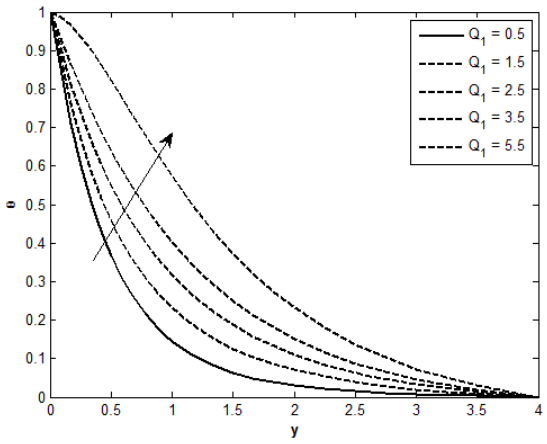

Figure 6 Temperature distribution for various values of Q1.

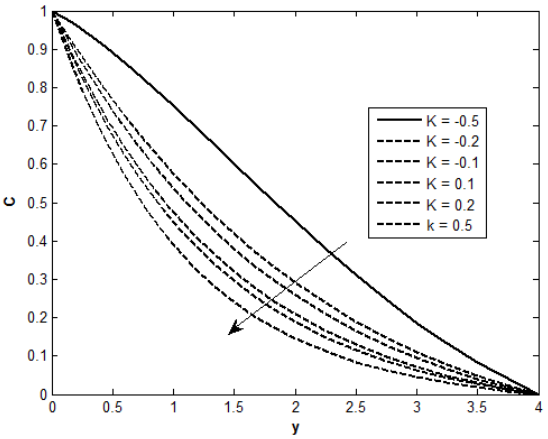

Figure 7 Concentration profiles for various values of K.

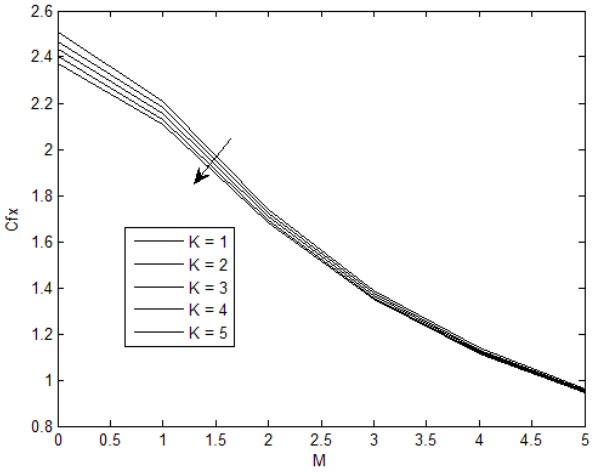

Figure 8 Effect of M on skin friction coefficient for various values of K.

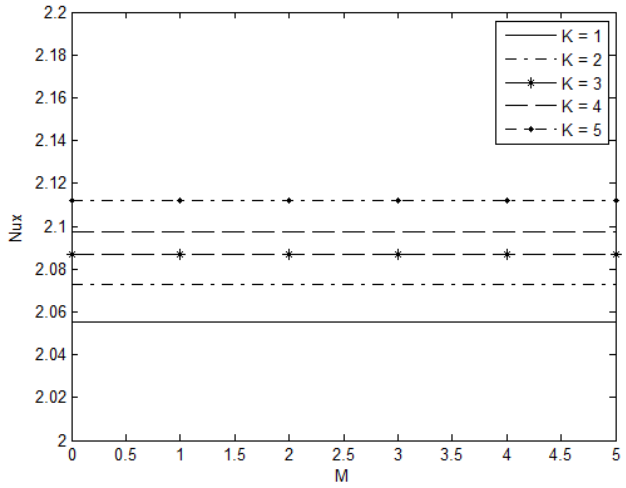

Figure 9 Effect of M on Nusselt number for various values of K.

Table 1 Numerical values of the Cfx and Nux/Rex for G=4, N=0.5, D-1=2, Pr=0.71, Ec=0.0001, Q¬1=0.5.

a	R	K	Sc	Cf_x	Nu_x/Re_x
2.0	3	0.5	0.6	1.6889	2.1589
1.0	3	0.5	0.6	1.5332	1.7608
1.0	3	-0.5	0.6	1.8849	1.9878
2.0	3	-0.5	0.4	2.2714	1.5212
1.0	1	-0.5	0.4	2.3848	1.2896

Table 2 Numerical values of the Cfx and Shx/Rex for G=4, N=0.5, D-1=2, Pr=0.71, Ec=0.0001, R=3, =2, Q¬1=0.5

Sc	K	C_{fx}	Sh_x/Re_x
0.4	0.5	1.5457	0.8097
0.4	1.0	1.9981	0.9699
0.6	1.5	1.4925	1.3757
0.6	-0.5	1.8289	0.1970
0.4	-1.0	2.2932	0.55

CONFLICT OF INTERESTS

None.

ACKNOWLEDGMENTS

None.

REFERENCES

W. Tan, T. Masuoka, Stokes first problem for a second grade fluid in a porous half-space with heated boundary, Int. J. Non- Linear Mech. 40 (2005) 515522.

M.M. Rashidi, S.A. Majid, A. Mostafa, Application of homotopy analysis method to the unsteady squeezing flow of a second-grade fluid between circular plates, Math. Probl. Eng. 18 (2010), 706840.

T. Hayat, M. Qasim, S.A. Shehzad, A. Alsaedi, Unsteady stagnation point flow of second grade fluid with variable free stream, Alexandria Eng. J. 53 (2014) 455461.

J. Hartmann, Hg-dynamics I theory of the laminar flow of an electrically conductive liquid in a homogenous magnetic field, Det Kongelige Danske Videnskabernes Selskab Mathematisk-fysiske Meddelser 15 (1937) 127.

V.V.S. Murty, A. Gupta, N. Mandloi, A. Shukla, Evaluation of thermal performance of heat exchanger unit for parabolic solar cooker for off-place cooking, Indian J. Pure Appl. Phys. 45 (2007) 745748.

N.K. Raja, M.S. Khalil, S.A. Masood, M. Shaheen, Design and manufacturing of parabolic trough solar collector system for a developing country Pakistan, J. Am. Sci. 7 (2011) 365372. [7] R. Muthucumaraswamy, E. Geetha, Effects of parabolic motion on an isothermal vertical plate with constant mass flux, Ain Shams Eng. J. 5 (2014) 13171323.

N.S. Akbar, S. Nadeem, R.U. Haq, S. Ye, MHD stagnation point flow of Carreau fluid toward a permeable shrinking sheet: dual solutions, Ain Shams Eng. J. 5 (2014) 12331239.

M. Sheikholeslami, D.D. Ganji, M. Gorji-Bandpy, Soheil Soleimani, Magnetic field effect on nanofluid flow and heat transfer using KKL model, J. Taiwan Inst. Chem. Eng. 45 (2014) 795807.

M. Sheikholeslami, D.D. Ganji, M.M. Rashidi, Magnetic field effect on unsteady nanofluid flow and heat transfer using Buongiorno model, J. Magn. Magn. Mater. 416 (2016) 164173.

M. Sheikholeslami, M. Gorji-Bandpy, D.D. Ganji, MHD free convection in an eccentric semi-annulus filled with nanofluid, J. Taiwan Inst. Chem. Eng. 45 (2014) 12041216.

M. Sheikholeslami, R. Ellahi, Three dimensional mesoscopic simulation of magnetic field effect on natural convection of nanofluid, Int. J. Heat Mass Transf. 89 (2015) 799808.

M. Sheikholeslami, K. Vajravelu, M.M. Rashidi, Forced convection heat transfer in a semi annulus under the influence of a variable magnetic field, Int. J. Heat Mass Transf. 92 (2016) 339348.

M. Sheikholeslami, A.J. Chamkha, Electrohydrodynamic free convection heat transfer of a nanofluid in a semi-annulus enclosure with a sinusoidal wall, Numer. Heat Transfer, Part A 69 (2016) 781793.

M.V. Krishna, A.J. Chamkha, Hall and ion slip effects on MHD rotating boundary layer flow of nanofluid past an infinite vertical plate embedded in a porous medium, Results in Physics 15 (2019), 102652, https://doi.org/10.1016/j.rinp.2019.102652.

M.V. Krishna, G.S. Reddy, A.J. Chamkha, Hall effects on unsteady MHD oscillatory free convective flow of second grade fluid through porous medium between two vertical plates, Physics of Fluids 30 (2018), 023106, https://doi.org/10.1063/ 1.5010863

M.V. Krishna, M.V. Chamkha, Hall effects on unsteady MHD flow of second grade fluid through porous medium with ramped wall temperature and ramped surface concentration, Physics of Fluids 30 (2018), 053101, https://doi.org/10.1063/ 1.5025542.

M. Sheikholeslami, D.D. Ganji, M.Y. Javed, R. Ellahi, Effect of thermal radiation parameter on magnetohydrodynamics nanofluid flow and heat transfer by means of two phase model, J. Magn. Magn. Mater. 374 (2015) 3643.

M.V. Krishna, K. Jyothi, A.J. Chamkha, Heat and mass transfer on unsteady, magnetohydrodynamic, oscillatory flow of second-grade fluid through a porous medium between two vertical plates, under the influence of fluctuating heat source/sink, and chemical reaction, Int. Jour. of Fluid Mech. Res. 45 (5) (2018) 459477, https://doi.org/10.1615/InterJFluidMechRes.2018024591.

H.R. Kataria, A.S. Mittal, Mathematical model for velocity and temperature of gravity-driven convective optically thick nanofluid flow past an oscillating vertical plate in presence of magnetic field and radiation, J. Nigerian Math. Soc. 34 (2015) 303317.

S. Nadeem, R.U. Haq, N.S. Akbar, Z.H. Khan, MHD threedimensional Casson fluid flow past a porous linearly stretching sheet, Alexandria Eng. J. 52 (2013) 577582.

H.R. Kataria, A.S. Mittal, Velocity, mass and temperature analysis of gravity-driven convection nanofluid flow past an oscillating vertical plate in presence of magnetic field in a porous medium, Appl. Therm. Eng. 110 (2017) 864–874.